

Detection prospects of light pseudoscalar Higgs boson at the LHC

MONORANJAN GUHAIT ^{*}, ARAVIND H. VIJAY [†] AND JACKY KUMAR [‡]

*Department of High Energy Physics,
Tata Institute of Fundamental Research,
Homi Bhabha Road, Mumbai-400005, India*

Abstract

The discovery potential of light pseudo scalar Higgs boson for the mass range 10-60 GeV is explored. In the context of the next-to-minimal supersymmetric standard(NMSSM) model, the branching fraction of light pseudo scalar Higgs boson decaying to a pair of photon can be quite large. A pair of light pseudo scalar Higgs boson produced indirectly through the standard model Higgs boson decay yields multiple photons in the final state and the corresponding production rate is restricted by ATLAS data. Discussing the impact of this constraint in the NMSSM, the detection prospects of light pseudoscalar Higgs boson in the channel consisting of at least three photons, a lepton and missing transverse energy are reported. It is observed that the possibilities of finding the pseudoscalar Higgs boson for the above mass range are promising for an integrated luminosity $\mathcal{L}=100 \text{ fb}^{-1}$ with moderate significances, which can reach to more than 5σ for higher luminosity options.

^{*}guchait@tifr.res.in

[†]arvind.vijay@tifr.res.in

[‡]jka@tifr.res.in

1 Introduction

The discovery of the Higgs boson of mass 125 GeV [1, 2] at the Large Hadron collider(LHC) by both the CMS and ATLAS experiments opens up a new window to study the physics beyond standard model (BSM). The current precision measurements of various properties of the Higgs boson, in particular couplings with fermions and gauge bosons indicate that it is indeed the candidate for the Standard model (SM) Higgs [3]. However, the possibility of interpreting it as the candidate of a BSM is not also ruled out completely. For example, the minimal supersymmetric standard model(MSSM), a candidate for BSM theories with two Higgs doublets leading to five physical Higgs boson states - h , H , A and H^\pm , where the first two are the CP-even, and others are the CP-odd and charged Higgs boson respectively, offers its lightest CP-even Higgs boson(h) as the candidate for the SM-like Higgs boson. Theoretically, in the MSSM, the mass of the Higgs boson, precisely the lightest state h , is connected with other sparticles strongly, in particular, with the third generation of squarks, through higher order corrections which enhance its tree level mass substantially. Consequently, the corresponding region of the parameter space is constrained owing to the larger mass of the Higgs boson. For instance, Higgs mass of 125 GeV requires, either a heavier mass of top squarks or a very large mixing in the top squark sector predicting lighter top squarks [4, 5]. Furthermore, the non-minimal variations of the MSSM with an extended Higgs sector, such as the next to Minimal supersymmetric standard model(NMSSM) [6–9] with an additional Higgs singlet field (S) in addition to two Higgs doublets, resulting in seven physical Higgs bosons, also can offer one of its CP even Higgs boson as the candidate for the SM-like Higgs with mass 125 GeV. Interestingly, in this case, one does not require so much fine tuning of the parameter space like the MSSM to accommodate the 125 GeV SM-like Higgs Boson [4, 10]. In general, two Higgs doublet models of various types contain potential features to interpret one of its CP even Higgs boson as the SM-like in the alignment limit along the direction of vacuum expectation values(VEV) of doublets [11–13]. Needless to say, that in all these cases, the BSM with extended Higgs sector predicts multiple Higgs boson states in addition to the SM-like one. Perhaps, discovery of an extra non-SM like Higgs boson might be one of the unambiguous signal to confirm the new physics model.

With this motivation, looking for the non-SM like Higgs boson at the LHC in the framework of the NMSSM has received a lot of attention since the discovery of the 125 GeV Higgs boson [14–28]. The enlarged Higgs sector of the NMSSM interpreting one of the CP even state as the SM-like Higgs, predicts lighter Higgs boson states, even much lower than 125 GeV for a wide region of parameters [24]. These lighter Higgs bosons are

not ruled out by any past experiments because of their suppressed couplings with gauge bosons and fermions. Many phenomenological studies exist in the literature regarding the searches of these lighter Higgs boson states at the LHC in the context of the NMSSM (see for details ref. [29] and references there in). On the experimental side, searching for these lighter Higgs boson states at the LHC is also one of the focused area since the discovery of the 125 GeV Higgs boson. For instance, CMS and ATLAS experiments published results on the searches of light Higgs bosons for various final states. The non observation of any signal event predicts the model independent exclusion of the Higgs production rate corresponding to that final state, for a given mass of the Higgs boson [30–33] Recasting these limits, possibly the parameter space of several models with extended Higgs can be constrained [34–36].

In this present study, we explore the discovery potential of light pseudo scalar Higgs boson(A_1) of mass less than $m_H/2$ at the LHC Run 2 experiment with the center of mass energy $\sqrt{S}=13$ TeV, where H represents the SM Higgs. As noted earlier, the direct production of these light singlet like Higgs boson state is suppressed due to the tiny couplings with the fermions. Alternatively, we consider the production of light A_1 indirectly via the decay of the SM Higgs boson as,

$$H \rightarrow A_1 A_1, \quad (1.1)$$

with the production of H via the standard mechanisms. It is to be noted here that the total branching ratio of the SM Higgs to undetected decay modes (BR_{BSM}) is restricted by Higgs data, and predicted to be [3],

$$BR_{BSM} \lesssim 0.34 \text{ at } 95\% \text{ C.L.} \quad (1.2)$$

Hence, the presence of non-SM decay modes of SM-like Higgs boson is not completely ruled out. Unlike the couplings of singlet like A_1 with the fermions, the tree level Higgs-to-Higgs coupling, H - A_1 - A_1 is not suppressed and widely varies with the model parameters [9], to be discussed in the next section.

The decay modes of light singlet like A_1 are very interesting. Due to the presence of finite fraction of doublet component in its physical state, A_1 dominantly decays via $A_1 \rightarrow b\bar{b}$, along with other sub-dominant channels such as, $\mu\mu, \tau\tau$. However, surprisingly, it is observed that corresponding to a certain kind of parameter space, the branching fraction (BR) of,

$$A_1 \rightarrow \gamma\gamma, \quad (1.3)$$

can be as large as 100%. This large BR of A_1 into this di-photon channel is a novel feature of the NMSSM unlike the other SUSY models [21, 23, 24, 37, 38]. Since experimentally, photon is a well reconstructed clean object, this di-photon mode is expected to provide a robust signal of A_1 at the LHC. Following this, we try to exploit this di-photon mode of A_1 , to find its discovery potential at the LHC Run 2 experiment. At the parton level, the production of a pair of A_1 via the (1.1), and its subsequent decay following the (1.3), results in four photons in the final state. Presence of multiple photons in the final state is of course, very encouraging, since the contamination due to the SM backgrounds is not expected to be severe [39–42]. In this present study, the production of the SM Higgs H is considered in association with top pairs($t\bar{t}H$), gauge bosons(WH , ZH) and also the single top quark(tH). In order to regulate the possible contamination due to the SM backgrounds, we demand at least one hard lepton arising from W or semileptonic decays of top quarks, in the final state along with at least three photons. The requirement of one lepton in the final state barring us from using the H production via gluon-gluon fusion, which is already analyzed and reported in the paper of Ref. [43].

Hence, the production mechanism of the signal, $n_\gamma\gamma + n_\ell\ell + \cancel{E}_T$ ($\ell = e, \mu$, $n_\gamma \geq 3$, $n_\ell \geq 1$) can be represented as,

$$\begin{aligned} pp &\rightarrow t\bar{t}H, WH, ZH, tH \\ &\rightarrow n_\gamma\gamma + n_\ell\ell + \cancel{E}_T \end{aligned} \quad (1.4)$$

with H and A_1 decays given by (1.1) and (1.3) respectively. The \cancel{E}_T arises due to the presence of neutrinos in the leptonic decays of W and top quarks. The sources of various possible backgrounds are discussed in the later section.

Notice that the signal rate depends on the product of BRs as,

$$\beta = \text{BR}(H \rightarrow A_1 A_1) \times \text{BR}(A_1 \rightarrow \gamma\gamma)^2. \quad (1.5)$$

Interestingly, this product of BRs is found to be constrained by ATLAS data published recently [33]. The ATLAS collaboration carried out searches for new phenomena in events with at least three photons at a center-of-mass energy 8 TeV with an integrated luminosity of 20.3fb^{-1} . From the non observation of any excess events, limits are set at 95% C.L on the rate of events in terms of cross section multiplied by branching ratios [33],

$$\sigma \times \beta \lesssim 10^{-3} \sigma_{SM}, \quad (1.6)$$

here σ is the Higgs production cross section in new physics scenario, where as σ_{SM} is

the same, but for the SM Higgs. The above constraint sets upper limit on β as,

$$\beta \lesssim 10^{-3}, \quad (1.7)$$

provided the Higgs in the context of new physics phenomena is the SM like Higgs boson of mass 125 GeV. Since our signal arises through the same decay channels, (1.1) and (1.3), therefore the corresponding rate is limited by the above constraint. Moreover, the region of the parameter space, and hence the corresponding BRs of the decay channels, ((1.1) and (1.3)), are also expected to be constrained, which are also investigated in this study. Considering all these restrictions, a detailed simulation of signal and backgrounds are carried out to find the discovery potential of A_1 at the LHC for few luminosity options.

We present our study as follows. Discussing the NMSSM model and decay modes of A_1 very briefly in Sec. (2), we present results of signal and background simulation in Sec. (3). Finally we summarize in Sec. (4).

2 The NMSSM

It is instructive to discuss qualitatively some features of the NMSSM in the context of this present study. As already mentioned, the Higgs sector in this model is extended by an additional Higgs field singlet under SM gauge transformation. Historically, this model was motivated to address the μ problem [44], where μ is defined to be the Higgsino mass parameter. Ideally, μ is free to take any value ranging from EW scale to Planck scale which is not such a favorable scenario. In order to cure this problem, the μ term is generated dynamically through the vacuum expectation value (vev) of the singlet field. In the \mathbb{Z}_3 invariant NMSSM, the superpotential with two Higgs doublets (H_u, H_d) and a singlet (S) Higgs field is of the form:

$$\mathcal{W}_{\text{NMSSM}} = \mathcal{W}_{\text{MSSM}}|_{\mu=0} + \lambda S H_u H_d + \frac{1}{3} \kappa S^3, \quad (2.1)$$

where λ and κ are the dimensionless couplings¹ and $\mathcal{W}_{\text{MSSM}}$ represents the superpotential in MSSM without μ term. Effect of Pecci-Quinn symmetry [46] is avoided adding the extra S^3 term to the potential. Once the singlet Higgs field receives vev (v_s), i.e., $\lambda S H_u H_d \sim \lambda v_s H_u H_d$, λv_s appears to be effective μ parameter. Alternate solutions also exist to address the μ problem [47, 48]. The presence of two Higgs doublets and one singlet field lead to seven physical Higgs bosons states, such as, 3 CP-even Higgs

¹Perturbative nature of couplings requires, $\lambda^2 + \kappa^2 < 0.7$ [45].

states H_1, H_2, H_3 (assuming $m_{H_1} < m_{H_2} < m_{H_3}$), 2 CP-odd states A_1, A_2 (assuming $m_{A_1} < m_{A_2}$) and two charged Higgs bosons [9]. Contribution due to the additional singlet-doublet mixing term $\lambda S H_u H_d$, enhances the tree level Higgs mass significantly reducing the need for large loop corrections to achieve its value 125 GeV. This extra tree level contribution is proportional to $\lambda v \sin 2\beta$, favoring lower value of $\tan \beta$ and larger value of λ , where $v = \sqrt{v_u^2 + v_d^2}$, with v_u and v_d are the vevs for up-type and down type Higgs doublets, and $\tan \beta$ is the ratio of these two vevs [7, 49–53]. The physical states, in particular, the neutral Higgses are composed of both doublet(H_u, H_d) and singlet component(S) resulting in a wider variation of their masses and coupling strength with fermions and gauge bosons. While offering one of the CP even Higgs as the SM-like 125 GeV Higgs, the other Higgs boson states can be very light. For instance, depending on the parameter space, if $H_1 \sim H$ ($H_2 \sim H$), then the A_1 (or both H_1 and A_1) can be very light, even much below than 100 GeV [14–16, 18, 19, 22–27]. Due to the presence of various decay channels of non-SM like Higgs bosons, such as, $b\bar{b}, \tau^+\tau^-, WW, ZZ, gg, c\bar{c}, \gamma\gamma$, and the wide variation of the corresponding BRs, the phenomenology of the Higgs sector in the NMSSM is very diverse [24]. Moreover, in particular, the Higgs to Higgs decays e.g. $H_1 \rightarrow A_1 A_1$, along with various other decay modes of A_1 provide more options to probe the NMSSM Higgs sector in colliders [54–57].

The parameter space sensitivity to the signal, (1.4) can be realized by looking into the structure of relevant couplings involving the decay channels, (1.1) and (1.3). Assuming A_1 is almost singlet like, the simpler form of tree level, H_1 - A_1 - A_1 coupling is given by,

$$g_{H_1-A_1-A_1} : \sqrt{2}v\lambda \{[\lambda (S_{11} \cos \beta + S_{12} \sin \beta)] + [\kappa (S_{12} \cos \beta + S_{11} \sin \beta)]\} \quad (2.2)$$

where S_{11} and S_{12} are components of H_d and H_u in the physical Higgs boson state. The more general structure of the couplings are shown in the Appendix. The above expression clearly shows the explicit dependence of $\text{BR}(H_1 \rightarrow A_1 A_1)$ on λ and κ . If this decay is kinematically allowed, then with the increase of λ , the corresponding BR goes up implying more restrictions on λ due to the upper bound on the SM Higgs BR for undetected decay channels, (1.7). Note that in the context of our study H_1 is SM-like Higgs boson i.e $H_1 \sim H$.

On the other hand, the reason of larger decay rate of A_1 to di-photon channel can be attributed to the singlet nature of A_1 , which leads to a very suppressed rate of the tree level decay modes, $A_1 \rightarrow b\bar{b}, \tau\bar{\tau}$, but an enhancement of the di-photon channel via chargino loop. Presence of a finite amount of Higgsino composition in the chargino state which is present in the loop leads to a coupling with singlet like A_1 causing this enhancement [26](see the Appendix for details). Hence, the suppression of tree level

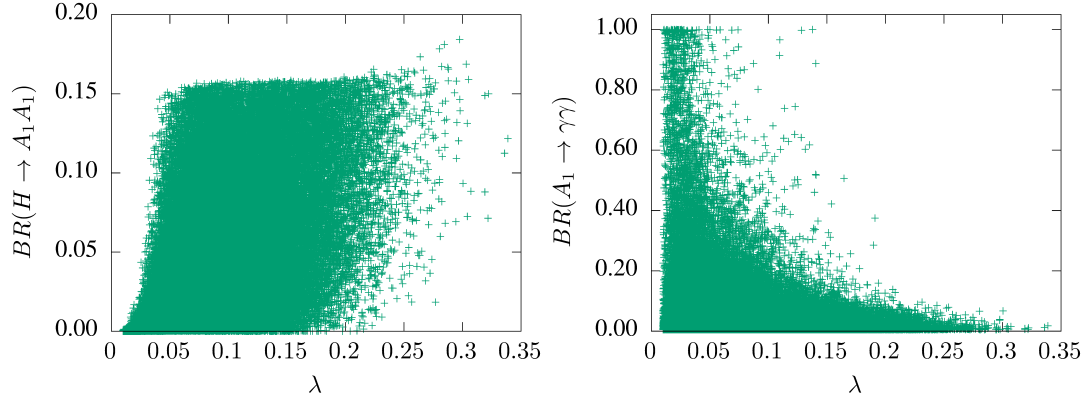


Figure 1: Allowed regions by all constraints. For details see the text.

decay modes to fermions and little enhancement of loop induced couplings of A_1 with photons results in a larger BR for the di-photon decay channel. A detailed study is carried out to identify the corresponding parameter space which offer this di-photon BR large [26]. It is observed that a reasonable range of λ ($\sim 0.1 - 0.4$) and κ ($\sim 0.1 - 0.65$) corresponding to a wide range of values of A_λ defined to be the trilinear Higgs soft breaking parameter and (lighter chargino masses ($\sim 200 - 700$ GeV $\sim \mu_{\text{eff}}$)) can provide large $\text{BR}(A_1 \rightarrow \gamma\gamma)$ [26]. While it is non trivial to find the signal of A_1 , but it appears as an unambiguous indication of the NMSSM like model. Recall, we mentioned that the constraints on β , (1.7), from ATLAS data, possibly can constrain the model parameters, in particular λ and κ . In order to identify the constrained region of the NMSSM model parameters, including constraint given by (1.7), we scan over all related parameters for a wide range using **NMSSMTools** [58]. The details of the parameters and the corresponding ranges for scanning are as shown in Table. 1. Here we have used

Table 1: Range of parameters and masses used for numerical scan. Energy units are in GeV.

$\lambda \in [0.01, 0.8]$	$\tan(\beta) \in [1.5, 40]$	$A_{E_3} = 1500$
$\kappa \in [0.1, 0.8]$	$M_1 \in [0, 1000]$	$M_{L_3} = 300$
$A_\lambda \in [100, 3000]$	$M_2 \in [100, 1000]$	$M_{E_3} = 300$
$A_\kappa \in [-20, 50]$	$M_3 = 1500$	$M_{Q_3} \in [800, 3000]$
$\mu_{\text{eff}} \in [100, 1000]$	$A_{U_3} \in [-3000, 3000]$	

the relations $A_{D_3} = A_{U_3}$, $M_{U_3} = M_{D_3} = M_{Q_3}$, $A_{E_1} = A_{E_2} = A_{E_3}$ and $M_{L_1} = M_{L_2} = M_{L_3}$. While scanning parameters, various experimental and theoretical constraints incorporated in **NMSSMTools** are tested. These constraints include those from flavor

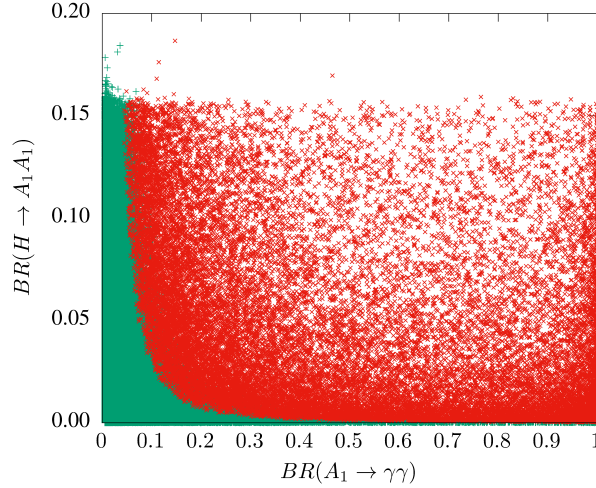


Figure 2: Allowed range of $BR(H_1 \rightarrow A_1 A_1)$ and $BR(A_1 \rightarrow \gamma\gamma)$. Red(Green) region is excluded(allowed) by the limit on β , (1.7).

Physics, limits on the masses of sparticles from LEP, Tevatron and LHC, precision measurements of Higgs properties and also the magnetic moment of muon, $g_\mu - 2$. It is to be noted that the constraint from the measurement of dark matter relic density is not taken into consideration. Fig. 1 presents the allowed range of $BR(H \rightarrow A_1 A_1)$ (left) and $BR(A_1 \rightarrow \gamma\gamma)$ (right) for various values of λ including ATLAS constraint, (1.7). Notice that the higher values of $(\lambda \gtrsim 0.35)$, which enhance the H_1 - A_1 - A_1 coupling((2.2)), and hence the corresponding BR, are not favored primarily due to Higgs data, (1.2). Remarkably, for the same range of λ , the $Br(A_1 \rightarrow \gamma\gamma)$ is found to be large, even as large as $\sim 100\%$. We observed that the impact of ATLAS constraint, (1.7) is not significant. However, we observe an interesting correlation of these two BRs, which is demonstrated in Fig. (2). The entire shaded region is excluded by all constraints including the ATLAS limit, (1.7), except the the green region which remains unconstrained. The notable feature of this plot is that the higher values of $BR(A_1 \rightarrow \gamma\gamma)$, even though predicted by the model are not favored by the current ATLAS data. For a larger range of $BR(H_1 \rightarrow A_1 A_1)$, smaller values of $BR(A_1 \rightarrow \gamma\gamma)$ are allowed and vice-versa. It is to be emphasized here that the restrictions of these two BRs along with their correlations are expected to affect future searches of light A_1 following these two decay channels.

3 Signal and Background

As discussed before, we focus on the signal final state consisting of at least three photons and one or more leptons along with missing transverse energy \cancel{E}_T , see (1.4). arising via

the associated production of SM Higgs following the decays, (1.1) and (6.3). The hard lepton comes from the W decay or semileptonic decay of top quark. In this context, we briefly discuss about the SM Higgs production cross section corresponding to our channels, (1.4). Currently, the $t\bar{t}H$ cross section in proton-proton collision is well understood upto next to leading(NLO) order including both QCD and EW correction. The QCD processes contribute dominantly to NLO correction [59–61], where as the size of the NLO electro-weak(EW) correction is about $\sim 1.7\%$ [62–64]. The total $t\bar{t}H$ cross section up to QCD NLO plus EW is found to be about 500 fb with K-factor 1.25 [65]. The dominant uncertainty is about $\sim 10\%$ arising mainly due to the variation of QCD scales. A fixed-order computation of the NNLO QCD correction is not easy to perform due to the technical difficulties. However, attempts are made to compute the NNLO QCD correction isolating a particular class of higher order diagrams, for instance, taking into account the effect of soft gluon emission beyond NLO [66,67]. It is found that this approximate NNLO correction reduces the systematic uncertainty in the total $t\bar{t}H$ production by a sizable amount($\sim 5\text{--}6\%$). However, in our estimation we use only NLO QCD+EW corrected total $t\bar{t}H$ cross section. We take into account the production of SM Higgs in association with a single top, $tH + \bar{t}H$. At LO, tH production takes place via both t-channel and s-channel Feynman diagrams in 4 flavor scheme (4FS) as well as 5FS [68]. In 4FS, the final state contains a b-quark or partons in association with tH pair, where as in 5FS, the gluon-bottom quark fusion produces the final state $tW^\pm H$ and tHq at the leading order. Up to NLO level, the t-channel, s-channel and W^\pm associated production can be distinguished in 5FS case, but in 4FS they interfere at higher order level, however, the effect of interference is too small to be significant. Since, we require one lepton in the final state, in our simulation we estimate contribution from all channels. In the 4FS the NLO $tH + \bar{t}H$ cross section is estimated to be 67.4 fb with an uncertainty about 1% due to the top mass and bottom quark mass uncertainty [65], where as in 5FS, the NLO cross section is about 74.4 fb with a K-factor 1.2 [65,68]. In our simulation we consider contribution due to the tHq productions in 5FS, and the s-channel production corresponding to the final states tHb and tHW^\pm . The theoretical prediction of the $W^\pm H, ZH$ production is currently available up to NNLO QCD including EW correction with an uncertainty at the level of few percent. The precise estimations of the total $W^\pm H$ and ZH production at 13 TeV are found to be 1.37 pb and 884 fb respectively at NNLO including both QCD and EW corrections [65].

The dominant SM background contribution are due to the processes:

$$pp \rightarrow W\gamma\gamma, Z\gamma\gamma, t\bar{t}\gamma\gamma, t\bar{t}\gamma\gamma\gamma, \quad (3.1)$$

Table 2: Production cross sections for signal and background processes

Process	$\sigma(\text{fb})$	Source
$t\bar{t}H$	507	[65]
$W^\pm H$	1420	[65]
ZH	884	[65]
tHq (5FS)	72.71	MG5NLO
tHb (s-channel)	2.82	MG5NLO
tHW^\pm (s-channel)	15.17	[65]
$W^\pm\gamma\gamma$	407	MG5NLO
$Z\gamma\gamma$	257	MG5NLO
$t\bar{t}\gamma\gamma\gamma$	0.67	MG5LO
$t\bar{t}\gamma\gamma$	13.64	MG5NLO

where lepton originates from W or semi-leptonic decay of top quark. In all the above hard processes, more number of hard γ may appear radiatively from the initial states. In addition lepton can fake also as a photon. We also checked the background contribution from $t\bar{t}H(\rightarrow \gamma\gamma)$ and found it to be very small to consider due to very tiny $\text{BR}(H \rightarrow \gamma\gamma)$ decay. The production cross sections for some of the processes described above are computed using `MadGraph5_aMC@NLO-2.4.3(MG5NLO)` [69] and presented in Table (2), which are subject to the following kinematic cuts on the transverse momentum and rapidity of leptons, photons and jets:

$$p_T^{\ell,\gamma} > 10 \text{ GeV}, \quad |\eta_{\ell,\gamma}| < 2.5 \quad (3.2)$$

$$p_T^j \geq 20 \text{ GeV}, \quad |\eta_j| < 5. \quad (3.3)$$

The NNPDF23LO parton distribution function [70] are chosen to provide input parton flux and setting factorization and renormalization scales to $\sqrt{\hat{s}}$, where \hat{s} is the energy in the parton center of mass frame. The cross section of $t\bar{t}\gamma\gamma$ is obtained at the NLO multiplying the k-factor 1.35 [69] with LO cross section given by MadGraph. The cross sections for the processes $t\bar{t}H$, $W^\pm H$ and ZH are taken from ref. [65]. The simulation is performed generating the matrix element using `MadGraph5_aMC@NLO-2.4.3` [69], and then for showering and hadronization passed through `PYTHIA8-8.2.19` [71]. Events are then stored in HepMC format using `HepMC-2.06.09` [72] in order to use `Delphes-3.3.3` [73] to take into account of detector effects. In Delphes simulation, we provide inputs through CMS data card setting, but changing the photon isolation criteria in order to

implement our strategy for its selection, as described later. We have also verified our results using ATLAS card and found its effect not to be very different. In the following, we describe briefly about the selection of objects in the simulation.

- **Lepton Selection:** Leptons are reconstructed parameterizing the reconstruction efficiencies as a function of both energy and momentum, and the final momentum obtained by a Gaussian smearing of the initial momentum. Both electrons and muons are selected, subject to cuts on the transverse momenta (p_T^ℓ) and pseudo rapidity (η^ℓ) as,

$$p_T^\ell \geq 20 \text{ GeV}, \quad |\eta^\ell| \leq 2.5, \quad (l = e, \mu), \quad (3.4)$$

Restriction on η^ℓ is due to the tracker coverage in the detector. The cleanliness of the lepton is ensured by measuring the hadronic activities around the lepton direction, requiring the total transverse energy,

$$E_T^{AC}(\ell) < 0.12 p_T^\ell, \quad (3.5)$$

where $E_T^{AC}(\ell)$ is the scalar sum of transverse energies of all particles with minimum transverse momentum 0.5 GeV around the lepton direction within a cone size of $\Delta R = 0.5$.

- **Photon selection:** In the Delphes, the genuine photons and electrons, which reach the electromagnetic calorimeter without any track - faking as photon, are considered. The conversions of photons into electrons and positrons pairs are neglected. The photons are selected with cuts,

$$p_T^\gamma > 20, 15, \quad |\eta_\gamma| < 2.4, \quad (3.6)$$

where, cut on leading and sub-leading photons are 20 GeV and 15 GeV respectively. Due to the presence of multiple photons in the signal events, isolation of it is checked in such a way that not many genuine photons are missed. In this regard, we closely follow the strategy adopted by ATLAS [33] to select isolated photons. First, we estimate the total transverse momentum(E_T^{AC}) of all particles within a region, $\Delta R < 0.4$, around the photon direction. In the next step, the E_T^{AC} is corrected by subtracted out the p_T of a genuine photon, if it is found within an annulus region $0.15 < \Delta R < 0.4$ around the photon direction. Finally, we require, $E_T^{AC} < 4$ GeV for photon isolation.

Table 3: Cross sections(σ) after each set of cuts normalizing it by acceptance efficiencies for three values of m_{A_1} (in GeV).

$\sigma(fb) \rightarrow$	$t\bar{t}H$ 507.1			$W^\pm H$ 1420			ZH 883.9		
	m_{A_1}			m_{A_1}			m_{A_1}		
Selection	10	30	60	10	30	60	10	30	60
$N_\gamma \geq 3$	105.8	142.7	192.8	355.0	429.7	620.6	17.6	20.8	29.2
$N_\ell \geq 1$	26.0	34.3	47.6	52.6	65.6	92.5	14.4	17.2	24.0
$\cancel{E}_T \geq 30$	22.2	29.6	40.8	36.3	47.0	65.0	0.9	1.2	1.8
$m_{\geq 3\gamma} < 130$	21.5	28.9	40.3	35.9	46.6	64.8	0.9	1.2	1.7

Table 4: Same as Table (3), but for tH process.

$\sigma(fb) \rightarrow$	tHb 2.82			tHj 72.71			tHW^\pm 15.17		
	m_{A_1}			m_{A_1}			m_{A_1}		
Selection	10	30	60	10	30	60	10	30	60
$N_\gamma \geq 3$	0.74	1.04	1.34	19.39	25.77	34.25	3.38	5.34	6.74
$N_\ell \geq 1$	0.09	0.13	0.18	2.48	3.51	4.60	0.90	1.42	1.76
$\cancel{E}_T \geq 30$	0.07	0.09	0.13	1.91	2.68	3.51	0.75	1.21	1.45
$m_{\geq 3\gamma} < 130$	0.07	0.09	0.13	1.90	2.66	3.47	0.73	1.19	1.43

- The missing transverse energy is estimated from the transverse component of the total energy deposited in the various components of the detector as

$$\vec{\cancel{E}}_T = - \sum \vec{p}_T(i), \quad (3.7)$$

i runs over all measured collection in the detector. A cut,

$$\cancel{E}_T > 30 \text{ GeV}. \quad (3.8)$$

is applied to select events.

Simulating signal and background processes implementing all selection cuts as described above, we estimate the signal significance for few integrated luminosity options, $\mathcal{L} = 100, 300, 1000 \text{ fb}^{-1}$. Before presenting the signal sensitivity, we discuss the effect of selection cuts showing event summary for both the signal in Tables. (3), (4) and

Table 5: Background cross section after each set of cuts normalizing it by acceptance efficiencies.

$\sigma(fb) \rightarrow$	$W\gamma\gamma$	$Z\gamma\gamma$	$t\bar{t}\gamma\gamma$	$t\bar{t}\gamma\gamma\gamma$
Selections	407.0	257.0	13.64	0.670
$N_\gamma \geq 3$	1.11	0.16	0.12	0.11
$N_\ell \geq 1$	0.089	0.081	0.024	0.028
$\cancel{E}_T > 30$	0.058	0.002	0.021	0.024
$m_{\geq 3\gamma} < 130$	0.026	0.001	0.007	0.007

backgrounds in (5). These tables show the cross sections times efficiency after each set of selection cuts as shown in the 1st column. The total production cross sections ($\sigma(fb)$) are shown for each of the processes. Three benchmark choices of $m_{A_1} = 10$ GeV, 30 GeV and 60 GeV are considered for the sake of presenting signal rates. Notice that, the photon selection cuts((3.6)), reduces the background contamination significantly, as clearly seen in Table (5). The missing transverse energy cut, (3.7), is very useful to suppress the $Z\gamma\gamma$ background, without much reduction in signal cross sections, except for the ZH case. Since, in both cases, due to the absence of genuine sources, the \cancel{E}_T is very soft, and hence affected drastically by a 30 GeV cut.

Furthermore, the invariant mass of the photon system originating from the SM Higgs decay of mass 125 GeV via a pair of light $A_1((1.1))$, is very effective in isolating backgrounds. Fig.(3) demonstrates the invariant mass spectrum of the photon system having at least three photons with selection cuts, (3.6), and for the values of $m_{A_1} = 10$ GeV and 40 GeV. For the sake of comparison, in the same figure, the dominant backgrounds due to $W\gamma\gamma$ and $t\bar{t}\gamma\gamma$ are also presented. This invariant mass is expected to be bounded by the mass of the Higgs boson, and it is clearly observed in Fig.(3). Obviously, a cut on the photon invariant mass $m_{n_\gamma\gamma} \lesssim 130$ GeV ($n_\gamma \geq 3$), shows an impressive discrimination between background and signal events, without affecting the latter too much, as presented in Tables (3), (4) and (5). Eventually, the total background cross section remains to be 0.041 fb, where almost 70% contribution is due to the $W\gamma\gamma$ process. In case of the signal, WH is the leading source followed by $t\bar{t}H$, where as the contributions due to ZH and tH are very tiny. Note that, while presenting the signal cross sections in Table (3) and (4) the product of two BRs, (1.1), and (6.3), which is essentially β , is not taken into account.

In Table (6), we present cross sections for the signal sensitivity for three values of

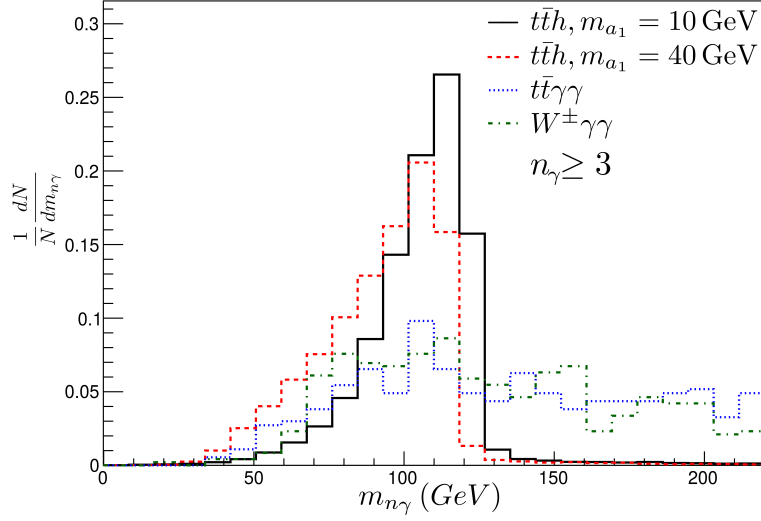


Figure 3: Invariant mass of photon system with at least three photons subject to photon selection cuts.

m_{A_1} along with the background cross section. Here the final signal cross sections are obtained by taking into account the depletion due to the BRs of Higgs and A_1 in terms of β , (1.5), which is restricted to be $\beta \lesssim 10^{-3}$, (1.7). We choose limiting value of $\beta = 10^{-3}$ to present signal significance in a model independent way. Three integrated luminosity options are considered, $\mathcal{L} = 100, 300, 1000 \text{ fb}^{-1}$ to present the discovery potential of A_1 . Signal sensitivity for lower masses of A_1 is moderate for 100fb^{-1} integrated luminosity, while for higher masses it is quite high. For higher luminosity options, the entire considered mass range of A_1 is easily detectable with significance more than 5σ . Although results are presented for three choices of m_{A_1} , however, conclusion remains same for the whole range of 10-60 GeV. The signal sensitivity degrades by 50% for a factor of two depletion of the limiting value of the combined branching ratio β . Note that this proposed search strategy does not work for lower masses ($\lesssim 10$ GeV) of A_1 , where one requires to develop different methodology due to the poor isolation of soft photons originating from very light A_1 decay [74]. Finally, as demonstrated, the discovery potential of light A_1 is quite high, even for 100fb^{-1} integrated luminosity option, which is expected to be achieved at the end of the next year LHC operation. Discovery of light A_1 , not only establish the new physics signal, but can also be an indication of the NMSSM model.

m_{A_1} (GeV)	Signal CS(fb)	Bkg CS(fb)	S/\sqrt{B} $\mathcal{L}(\text{fb}^{-1})$		
			100	300	1000
10	0.061	0.041	3.01	5.21	9.51
30	0.081		3.97	6.88	12.57
60	0.111		5.51	9.53	17.41

Table 6: Signal significance for three values of m_{A_1} with $\beta = 10^{-3}$ (see (1.5)).

4 Summary

The discovery potential of light pseudo scalar Higgs boson, A_1 of mass less than the half of the SM-like Higgs boson is investigated at the LHC Run 2 experiment. The light Higgs bosons are predicted by the NMSSM in addition to the SM-like Higgs boson of mass 125 GeV. In this model, the singlet like light pseudo scalar Higgs boson is found to be decaying to a pair of photons with a substantial BR. Numerous studies are already carried out by CMS and ATLAS collaborations to search for these light Higgs boson in various final states. In the absence of any signal, limits on the event rates are presented, and those can be translated to constrain the cross section times BRs corresponding to that final state for a given model framework. The recent published results by ATLAS in the context of new physics searches with the final state consisting of at least three photons impose a stringent constraint on the combination of $\text{BR}(H \rightarrow A_1 A_1)$ and $\text{BR}(A_1 \rightarrow \gamma\gamma)$, defined to be β in (1.5). In the context of the NMSSM model, a significant range of $\text{BR}(H \rightarrow A_1 A_1)$ and $\text{BR}(A_1 \rightarrow \gamma\gamma)$ are excluded for a moderate range of λ , a very sensitive parameter related to these decay modes. Moreover, we observe that higher range of $\lambda \gtrsim 0.35$ is disfavored for the parameter space where the SM-like Higgs is kinematically allowed to decay to a pair of A_1 . We explore the detection prospect of A_1 exploiting its di-photon decay channel focusing the final state having at least three photons accompanied with one or more hard leptons and missing transverse energy. The rate of signal event production is limited by β (1.7), due to ATLAS data, and is taken into account in our simulation. Carrying out a detailed simulation for signal and background processes including detector effects, and considering the limiting value of $\beta \lesssim 10^{-3}$, we present model independent significance for three integrated luminosity options. The detection prospects of light pseudo scalar Higgs boson for the above mass range is modest for 100 fb^{-1} integrated luminosity. However, with high integrated luminosity option, $\mathcal{L}=300\text{fb}^{-1}$ or more, the discovery potential is observed to be quite

rich with significance more than 5σ . In summary, we conclude that the discovery of A_1 in the diphoton channel will confirm not only the presence of new physics model, but more importantly, can be a characteristic signal of the NMSSM.

5 Acknowledgement

The authors are thankful to Ushoshi Maitra and Disha Bhatia who had collaborated at the initial phase of this work.

6 Appendix

H_1 - A_1 - A_1 coupling: The mass matrices for CP-even and CP-odd Higgses in the framework of the NMSSM can be diagonalized by orthogonal rotation matrices $S_{3\times 3}$ and $P_{3\times 3}$ respectively. The transformation from the weak basis states $H_i^s = (H_{dR}, H_{uR}, S_R)$ and $H_i^a = (H_{dI}, H_{uI}, S_I)$ to mass basis are given in terms of mixing matrix elements [9]

$$H_i = S_{ij}H_i^s, \quad A_i = P_{ij}H_i^a; \quad i, j = 1, 2, 3. \quad (6.1)$$

The Higgs couplings are very sensitive to these elements of the mixing matrices S_{ij} and P_{ij} .

Assuming the H_1 is SM-like, i.e singlet component ($S_{13} \sim 0$) is almost negligible, and A_1 state singlet like, i.e $P_{12}, P_{22} \sim 0$, the coupling structure of $H_1 - A_1 - A_1$ can be written as [9],

$$g_{H_1-A_1-A_1} \sim \frac{\lambda^2}{2} [v_d \Pi_{111}^{133} + v_u \Pi_{111}^{233}] + \frac{\lambda\kappa}{\sqrt{2}} [v_d \Pi_{111}^{233} + v_u \Pi_{111}^{133}]$$

where $\Pi_{111}^{333} = 2S_{i1}P_{13}^2$. For pure singlet state, $P_{13} \sim 1$, it turns out,

$$g_{H_1-A_1-A_1} \sim \sqrt{2}v\lambda \{[\lambda (\cos \beta S_{11} + \sin \beta S_{12})] + [\kappa (\cos \beta S_{12} + \sin \beta S_{11})]\} \quad (6.2)$$

with $\tan \beta = v_u/v_d$.

A_1 - γ - γ coupling: This coupling occurs at the loop level and for the singlet dominated A_1 , the chargino contribution is the dominant one. The partial decay width of $A_1 \rightarrow \gamma\gamma$ is given as [75, 76],

$$\Gamma(A_1 \rightarrow \gamma\gamma) = \frac{G_F \alpha_{em}^2 M_{A_1}^3}{32\sqrt{2}\pi^3} \left| \sum_f N_c e_f^2 g_f^{A_1} A_f(\tau_f) + \sum_{\tilde{\chi}_i^\pm} g_{\tilde{\chi}_i^\pm}^{A_1} A_{\tilde{\chi}_i^\pm}(\tau_{\tilde{\chi}_i^\pm}) \right|^2. \quad (6.3)$$

Here N_c is the QCD color factor, e_f is the electric charge of the fermions (f), $A_x(\tau_x)$ are the loop functions given by,

$$A_x(\tau_x) = \tau_x \left(\sin^{-1} \frac{1}{\sqrt{\tau_x}} \right)^2, \quad \tau_x = \frac{4M_x^2}{M_{A_1}^2}; \quad x = f, \tilde{\chi}_i^\pm. \quad (6.4)$$

Here $g_f^{A_1}$ are the couplings of A_1 with the heavier fermions ($f = t, b$) whereas $g_{\tilde{\chi}^\pm}^{A_1}$ represents its couplings with the charginos, these are given by [9],

$$\begin{aligned} g_u^{A_1} &= -i \frac{m_u}{\sqrt{2}v \sin \beta} P_{12}, \\ g_d^{A_1} &= i \frac{m_d}{\sqrt{2}v \cos \beta} P_{11}, \\ g_{\tilde{\chi}_i^\pm \tilde{\chi}_j^\mp}^{A_1} &= \frac{i}{\sqrt{2}} [\lambda P_{13} U_{i2} V_{j2} - g_2 (P_{12} U_{i1} V_{j2} + P_{11} U_{i2} V_{j1})] \end{aligned} \quad (6.5)$$

Here U and V are the chargino mixing matrices. In the pure singlet limit of A_1 the mixing elements P_{11} and $P_{12} \sim 0$ and hence the fermion couplings $g_u^{A_1}$ and $g_d^{A_1}$ are very small $\sim 10^{-5}$. Hence, corresponding fermionic loop contribution in (6.3) are extremely small. On the other hand, the presence of Higgsino composition in the chargino state yields a favorable coupling with A_1 via the singlet-Higgsino-Higgsino interaction [26].

References

- [1] **ATLAS Collaboration** Collaboration, G. Aad *et al.*, “Observation of a new particle in the search for the Standard Model Higgs boson with the ATLAS detector at the LHC,” *Phys.Lett.* **B716** (2012) 1–29, [arXiv:1207.7214](https://arxiv.org/abs/1207.7214) [hep-ex]. <https://arxiv.org/abs/1207.7214>.
- [2] **CMS Collaboration** Collaboration, S. Chatrchyan *et al.*, “Observation of a new boson at a mass of 125 GeV with the CMS experiment at the LHC,” *Phys.Lett.* **B716** (2012) 30–61, [arXiv:1207.7235](https://arxiv.org/abs/1207.7235) [hep-ex]. <https://arxiv.org/abs/1207.7235>.
- [3] **ATLAS, CMS Collaboration**, G. Aad *et al.*, “Measurements of the Higgs boson production and decay rates and constraints on its couplings from a combined ATLAS and CMS analysis of the LHC pp collision data at $\sqrt{s} = 7$ and 8 TeV,” *JHEP* **08** (2016) 045, [arXiv:1606.02266](https://arxiv.org/abs/1606.02266) [hep-ex].
- [4] L. J. Hall, D. Pinner, and J. T. Ruderman, “A Natural SUSY Higgs Near 126 GeV,” *JHEP* **04** (2012) 131, [arXiv:1112.2703](https://arxiv.org/abs/1112.2703) [hep-ph].

- [5] A. Arbey, M. Battaglia, A. Djouadi, F. Mahmoudi, and J. Quevillon, “Implications of a 125 GeV Higgs for supersymmetric models,” *Phys. Lett.* **B708** (2012) 162–169, [arXiv:1112.3028 \[hep-ph\]](#).
- [6] P. Fayet, “Supergauge Invariant Extension of the Higgs Mechanism and a Model for the electron and Its Neutrino,” *Nucl. Phys.* **B90** (1975) 104–124.
- [7] J. R. Ellis, J. Gunion, H. E. Haber, L. Roszkowski, and F. Zwirner, “Higgs Bosons in a Nonminimal Supersymmetric Model,” *Phys.Rev.* **D39** (1989) 844.
- [8] M. DREES, “Supersymmetric models with extended higgs sector,” *International Journal of Modern Physics A* **04** no. 14, (1989) 3635–3651, <http://www.worldscientific.com/doi/pdf/10.1142/S0217751X89001448>, <http://www.worldscientific.com/doi/abs/10.1142/S0217751X89001448>.
- [9] U. Ellwanger, C. Hugonie, and A. M. Teixeira, “The Next-to-Minimal Supersymmetric Standard Model,” *Phys. Rept.* **496** (2010) 1–77, [arXiv:0910.1785 \[hep-ph\]](#).
- [10] J.-J. Cao, Z.-X. Heng, J. M. Yang, Y.-M. Zhang, and J.-Y. Zhu, “A SM-like Higgs near 125 GeV in low energy SUSY: a comparative study for MSSM and NMSSM,” *JHEP* **03** (2012) 086, [arXiv:1202.5821 \[hep-ph\]](#).
- [11] H. E. Haber and D. O’Neil, “Basis-independent methods for the two-Higgs-doublet model. II. The Significance of $\tan\beta$,” *Phys. Rev.* **D74** (2006) 015018, [arXiv:hep-ph/0602242 \[hep-ph\]](#). [Erratum: *Phys. Rev.* **D74**, no. 5, 059905 (2006)].
- [12] J. Bernon, J. F. Gunion, H. E. Haber, Y. Jiang, and S. Kraml, “Scrutinizing the alignment limit in two-Higgs-doublet models: $m_h=125$ GeV,” *Phys. Rev.* **D92** no. 7, (2015) 075004, [arXiv:1507.00933 \[hep-ph\]](#).
- [13] J. Bernon, J. F. Gunion, H. E. Haber, Y. Jiang, and S. Kraml, “Scrutinizing the alignment limit in two-Higgs-doublet models. II. $m_H=125$ GeV,” *Phys. Rev.* **D93** no. 3, (2016) 035027, [arXiv:1511.03682 \[hep-ph\]](#).
- [14] A. Djouadi *et al.*, “Benchmark scenarios for the NMSSM,” *JHEP* **07** (2008) 002, [arXiv:0801.4321 \[hep-ph\]](#).
- [15] S. Heinemeyer, O. Stal, and G. Weiglein, “Interpreting the LHC Higgs Search Results in the MSSM,” *Phys. Lett.* **B710** (2012) 201–206, [arXiv:1112.3026 \[hep-ph\]](#).

- [16] S. F. King, M. Muhlleitner, and R. Nevzorov, “NMSSM Higgs Benchmarks Near 125 GeV,” *Nucl. Phys.* **B860** (2012) 207–244, [arXiv:1201.2671 \[hep-ph\]](#).
- [17] K. Agashe, Y. Cui, and R. Franceschini, “Natural Islands for a 125 GeV Higgs in the scale-invariant NMSSM,” *JHEP* **02** (2013) 031, [arXiv:1209.2115 \[hep-ph\]](#).
- [18] S. F. King, M. Mühlleitner, R. Nevzorov, and K. Walz, “Natural NMSSM Higgs Bosons,” *Nucl. Phys.* **B870** (2013) 323–352, [arXiv:1211.5074 \[hep-ph\]](#).
- [19] D. Albornoz Vasquez, G. Belanger, C. Boehm, J. Da Silva, P. Richardson, and C. Wymant, “The 125 GeV Higgs in the NMSSM in light of LHC results and astrophysics constraints,” *Phys. Rev.* **D86** (2012) 035023, [arXiv:1203.3446 \[hep-ph\]](#).
- [20] R. Barbieri, D. Buttazzo, K. Kannike, F. Sala, and A. Tesi, “Exploring the Higgs sector of a most natural NMSSM,” *Phys. Rev.* **D87** no. 11, (2013) 115018, [arXiv:1304.3670 \[hep-ph\]](#).
- [21] M. Badziak, M. Olechowski, and S. Pokorski, “New Regions in the NMSSM with a 125 GeV Higgs,” *JHEP* **06** (2013) 043, [arXiv:1304.5437 \[hep-ph\]](#).
- [22] J. Cao, F. Ding, C. Han, J. M. Yang, and J. Zhu, “A light Higgs scalar in the NMSSM confronted with the latest LHC Higgs data,” *JHEP* **11** (2013) 018, [arXiv:1309.4939 \[hep-ph\]](#).
- [23] N. D. Christensen, T. Han, Z. Liu, and S. Su, “Low-Mass Higgs Bosons in the NMSSM and Their LHC Implications,” *JHEP* **08** (2013) 019, [arXiv:1303.2113 \[hep-ph\]](#).
- [24] M. Guchait and J. Kumar, “Light Higgs Bosons in NMSSM at the LHC,” *Int. J. Mod. Phys.* **A31** no. 12, (2016) 1650069, [arXiv:1509.02452 \[hep-ph\]](#).
- [25] F. Domingo and G. Weiglein, “NMSSM interpretations of the observed Higgs signal,” *JHEP* **04** (2016) 095, [arXiv:1509.07283 \[hep-ph\]](#).
- [26] M. Guchait and J. Kumar, “Diphoton Signal of light pseudoscalar in NMSSM at the LHC,” *Phys. Rev.* **D95** no. 3, (2017) 035036, [arXiv:1608.05693 \[hep-ph\]](#).
- [27] J. Kumar and M. Paraskevas, “Distinguishing between MSSM and NMSSM through $\Delta F = 2$ processes,” *JHEP* **10** (2016) 134, [arXiv:1608.08794 \[hep-ph\]](#).

- [28] J. Kozaczuk and T. A. W. Martin, “Extending lhc coverage to light pseudoscalar mediators and coy dark sectors,” *Journal of High Energy Physics* **2015** no. 4, (2015) 46. [http://dx.doi.org/10.1007/JHEP04\(2015\)046](http://dx.doi.org/10.1007/JHEP04(2015)046).
- [29] U. Ellwanger, “Higgs Bosons in the Next-to-Minimal Supersymmetric Standard Model at the LHC,” *Eur. Phys. J.* **C71** (2011) 1782, [arXiv:1108.0157 \[hep-ph\]](#).
- [30] **CMS Collaboration**, S. Chatrchyan *et al.*, “Search for a light pseudoscalar Higgs boson in the dimuon decay channel in pp collisions at $\sqrt{s} = 7$ TeV,” *Phys. Rev. Lett.* **109** (2012) 121801, [arXiv:1206.6326 \[hep-ex\]](#).
- [31] **CMS Collaboration** Collaboration, C. Veelken, “Searches for MSSM and NMSSM Higgs bosons with the CMS detector,” Tech. Rep. CMS-CR-2014-260, CERN, Geneva, Oct, 2014. <https://cds.cern.ch/record/1953441>.
- [32] **CMS Collaboration**, V. Khachatryan *et al.*, “Search for a very light NMSSM Higgs boson produced in decays of the 125 GeV scalar boson and decaying into τ leptons in pp collisions at $\sqrt{s} = 8$ TeV,” *JHEP* **01** (2016) 079, [arXiv:1510.06534 \[hep-ex\]](#).
- [33] **ATLAS Collaboration**, G. Aad *et al.*, “Search for new phenomena in events with at least three photons collected in pp collisions at $\sqrt{s} = 8$ TeV with the ATLAS detector,” *Eur. Phys. J.* **C76** no. 4, (2016) 210, [arXiv:1509.05051 \[hep-ex\]](#).
- [34] G. Cacciapaglia, A. Deandrea, S. Gascon-Shotkin, S. Le Corre, M. Lethuillier, and J. Tao, “Search for a lighter Higgs boson in Two Higgs Doublet Models,” *JHEP* **12** (2016) 068, [arXiv:1607.08653 \[hep-ph\]](#).
- [35] R. Aggleton, D. Barducci, N.-E. Bomark, S. Moretti, and C. Shepherd-Themistocleous, “Review of LHC experimental results on low mass bosons in multi Higgs models,” *JHEP* **02** (2017) 035, [arXiv:1609.06089 \[hep-ph\]](#).
- [36] D. Bhatia, U. Maitra, and S. Niyogi, “Discovery prospects of Light Higgs at LHC in Type-I 2HDM,” [arXiv:1704.07850 \[hep-ph\]](#).
- [37] R. Dermisek and J. F. Gunion, “The NMSSM Solution to the Fine-Tuning Problem, Precision Electroweak Constraints and the Largest LEP Higgs Event Excess,” *Phys. Rev.* **D76** (2007) 095006, [arXiv:0705.4387 \[hep-ph\]](#).

- [38] U. Ellwanger, “A Higgs boson near 125 GeV with enhanced di-photon signal in the NMSSM,” *JHEP* **03** (2012) 044, [arXiv:1112.3548 \[hep-ph\]](#).
- [39] S. Moretti and S. Munir, “Di-photon Higgs signals at the LHC in the next-to-minimal supersymmetric standard model,” *Eur. Phys. J.* **C47** (2006) 791–803, [arXiv:hep-ph/0603085 \[hep-ph\]](#).
- [40] A. Arhrib, K. Cheung, T.-J. Hou, and K.-W. Song, “Associated production of a light pseudoscalar Higgs boson with a chargino pair in the NMSSM,” *JHEP* **03** (2007) 073, [arXiv:hep-ph/0606114 \[hep-ph\]](#).
- [41] M. Badziak, M. Olechowski, and S. Pokorski, “125 GeV Higgs and enhanced diphoton signal of a light singlet-like scalar in NMSSM,” *PoS EPS-HEP2013* (2013) 257, [arXiv:1310.4518 \[hep-ph\]](#).
- [42] U. Ellwanger and M. Rodriguez-Vazquez, “Discovery Prospects of a Light Scalar in the NMSSM,” *JHEP* **02** (2016) 096, [arXiv:1512.04281 \[hep-ph\]](#).
- [43] S. Chang, P. J. Fox, and N. Weiner, “Visible Cascade Higgs Decays to Four Photons at Hadron Colliders,” *Phys. Rev. Lett.* **98** (2007) 111802, [arXiv:hep-ph/0608310 \[hep-ph\]](#).
- [44] J. E. Kim and H. P. Nilles, “The mu Problem and the Strong CP Problem,” *Phys. Lett.* **B138** (1984) 150–154.
- [45] D. Miller, R. Nevzorov, and P. Zerwas, “The Higgs sector of the next-to-minimal supersymmetric standard model,” *Nucl. Phys.* **B681** (2004) 3–30, [arXiv:hep-ph/0304049 \[hep-ph\]](#).
- [46] R. Peccei and H. R. Quinn, “CP Conservation in the Presence of Instantons,” *Phys. Rev. Lett.* **38** (1977) 1440–1443.
- [47] G. F. Giudice and A. Masiero, “A Natural Solution to the mu Problem in Supergravity Theories,” *Phys. Lett.* **B206** (1988) 480–484.
- [48] A. E. Nelson and T. S. Roy, “New Supersoft Supersymmetry Breaking Operators and a Solution to the μ Problem,” *Phys. Rev. Lett.* **114** (2015) 201802, [arXiv:1501.03251 \[hep-ph\]](#).
- [49] M. Drees, “Supersymmetric Models with Extended Higgs Sector,” *Int. J. Mod. Phys.* **A4** (1989) 3635.

- [50] F. Franke and H. Fraas, “Neutralinos and Higgs bosons in the next-to-minimal supersymmetric standard model,” *Int.J.Mod.Phys.* **A12** (1997) 479–534, [arXiv:hep-ph/9512366](#) [hep-ph].
- [51] U. Ellwanger, M. Rausch de Traubenberg, and C. A. Savoy, “Particle spectrum in supersymmetric models with a gauge singlet,” *Phys.Lett.* **B315** (1993) 331–337, [arXiv:hep-ph/9307322](#) [hep-ph].
- [52] S. King and P. White, “Resolving the constrained minimal and next-to-minimal supersymmetric standard models,” *Phys.Rev.* **D52** (1995) 4183–4216, [arXiv:hep-ph/9505326](#) [hep-ph].
- [53] P. Drechsel, L. Galeta, S. Heinemeyer, and G. Weiglein, “Precise Predictions for the Higgs-Boson Masses in the NMSSM,” *Eur. Phys. J.* **C77** no. 1, (2017) 42, [arXiv:1601.08100](#) [hep-ph].
- [54] M. M. Almarashi and S. Moretti, “Low Mass Higgs signals at the LHC in the Next-to-Minimal Supersymmetric Standard Model,” *Eur. Phys. J.* **C71** (2011) 1618, [arXiv:1011.6547](#) [hep-ph].
- [55] A. Belyaev, J. Pivarski, A. Safonov, S. Senkin, and A. Tatarinov, “LHC discovery potential of the lightest NMSSM Higgs in the $h1 \rightarrow a1 a1 \rightarrow 4$ muons channel,” *Phys. Rev.* **D81** (2010) 075021, [arXiv:1002.1956](#) [hep-ph].
- [56] M. Almarashi and S. Moretti, “Very Light CP-odd Higgs bosons of the NMSSM at the LHC in 4b-quark final states,” *Phys. Rev.* **D84** (2011) 015014, [arXiv:1105.4191](#) [hep-ph].
- [57] N.-E. Bomark, S. Moretti, and L. Roszkowski, “Detection prospects of light NMSSM Higgs pseudoscalar via cascades of heavier scalars from vector boson fusion and Higgs-strahlung,” *J. Phys.* **G43** no. 10, (2016) 105003, [arXiv:1503.04228](#) [hep-ph].
- [58] U. Ellwanger, J. F. Gunion, and C. Hugonie, “NMHDECAY: A Fortran code for the Higgs masses, couplings and decay widths in the NMSSM,” *JHEP* **02** (2005) 066, [arXiv:hep-ph/0406215](#) [hep-ph].
- [59] S. Dawson, C. Jackson, L. H. Orr, L. Reina, and D. Wackeroth, “Associated Higgs production with top quarks at the large hadron collider: NLO QCD corrections,” *Phys. Rev.* **D68** (2003) 034022, [arXiv:hep-ph/0305087](#) [hep-ph].

- [60] S. Dawson, L. H. Orr, L. Reina, and D. Wackeroth, “Associated top quark Higgs boson production at the LHC,” *Phys. Rev.* **D67** (2003) 071503, [arXiv:hep-ph/0211438](#) [[hep-ph](#)].
- [61] L. Reina and S. Dawson, “Next-to-leading order results for t anti- t h production at the Tevatron,” *Phys. Rev. Lett.* **87** (2001) 201804, [arXiv:hep-ph/0107101](#) [[hep-ph](#)].
- [62] S. Frixione, V. Hirschi, D. Pagani, H. S. Shao, and M. Zaro, “Electroweak and QCD corrections to top-pair hadroproduction in association with heavy bosons,” *JHEP* **06** (2015) 184, [arXiv:1504.03446](#) [[hep-ph](#)].
- [63] S. Frixione, V. Hirschi, D. Pagani, H. S. Shao, and M. Zaro, “Weak corrections to Higgs hadroproduction in association with a top-quark pair,” *JHEP* **09** (2014) 065, [arXiv:1407.0823](#) [[hep-ph](#)].
- [64] Y. Zhang, W.-G. Ma, R.-Y. Zhang, C. Chen, and L. Guo, “QCD NLO and EW NLO corrections to $t\bar{t}H$ production with top quark decays at hadron collider,” *Phys. Lett.* **B738** (2014) 1–5, [arXiv:1407.1110](#) [[hep-ph](#)].
- [65] **LHC Higgs Cross Section Working Group** Collaboration, D. de Florian *et al.*, “Handbook of LHC Higgs Cross Sections: 4. Deciphering the Nature of the Higgs Sector,” [arXiv:1610.07922](#) [[hep-ph](#)].
- [66] A. Broggio, A. Ferroglia, B. D. Pecjak, A. Signer, and L. L. Yang, “Associated production of a top pair and a Higgs boson beyond NLO,” *JHEP* **03** (2016) 124, [arXiv:1510.01914](#) [[hep-ph](#)].
- [67] A. Kulesza, L. Motyka, T. Stebel, and V. Theeuwes, “Soft gluon resummation for associated $t\bar{t}H$ production at the LHC,” *JHEP* **03** (2016) 065, [arXiv:1509.02780](#) [[hep-ph](#)].
- [68] F. Demartin, F. Maltoni, K. Mawatari, and M. Zaro, “Higgs production in association with a single top quark at the LHC,” *Eur. Phys. J.* **C75** no. 6, (2015) 267, [arXiv:1504.00611](#) [[hep-ph](#)].
- [69] J. Alwall, R. Frederix, S. Frixione, V. Hirschi, F. Maltoni, O. Mattelaer, H. S. Shao, T. Stelzer, P. Torrielli, and M. Zaro, “The automated computation of tree-level and next-to-leading order differential cross sections, and their matching to parton shower simulations,” *JHEP* **07** (2014) 079, [arXiv:1405.0301](#) [[hep-ph](#)].

- [70] R. D. Ball, L. Del Debbio, S. Forte, A. Guffanti, J. I. Latorre, J. Rojo, and M. Ubiali, “A first unbiased global NLO determination of parton distributions and their uncertainties,” *Nucl. Phys.* **B838** (2010) 136–206, [arXiv:1002.4407 \[hep-ph\]](#).
- [71] T. Sjostrand, S. Mrenna, and P. Z. Skands, “PYTHIA 6.4 Physics and Manual,” *JHEP* **05** (2006) 026, [arXiv:hep-ph/0603175 \[hep-ph\]](#).
- [72] M. Dobbbs and J. B. Hansen, “The HepMC C++ Monte Carlo event record for High Energy Physics,” *Comput. Phys. Commun.* **134** (2001) 41–46.
- [73] **DELPHES 3** Collaboration, J. de Favereau, C. Delaere, P. Demin, A. Giammanco, V. Lemaître, A. Mertens, and M. Selvaggi, “DELPHES 3, A modular framework for fast simulation of a generic collider experiment,” *JHEP* **02** (2014) 057, [arXiv:1307.6346 \[hep-ex\]](#).
- [74] B. A. Dobrescu, G. L. Landsberg, and K. T. Matchev, “Higgs boson decays to CP odd scalars at the Tevatron and beyond,” *Phys. Rev.* **D63** (2001) 075003, [arXiv:hep-ph/0005308 \[hep-ph\]](#).
- [75] M. Spira, A. Djouadi, D. Graudenz, and P. M. Zerwas, “Higgs boson production at the LHC,” *Nucl. Phys.* **B453** (1995) 17–82, [arXiv:hep-ph/9504378 \[hep-ph\]](#).
- [76] M. Spira, “QCD effects in Higgs physics,” *Fortsch. Phys.* **46** (1998) 203–284, [arXiv:hep-ph/9705337 \[hep-ph\]](#).